SI Appendix, Material and Methods

A unique surface on Pat1 C-terminal domain directly interacts with Dcp2 decapping enzyme and Xrn1 5'-3' mRNA exonuclease in yeast

Clément Charenton[1], Claudine Gaudon-Plesse[2-5], Zaineb Fourati[1], Valerio Taverniti[2-5], Régis Back[1], Olga Kolesnikova[2-5], Bertrand Séraphin[2-5], Marc Graille[1]

[1] Laboratoire de Biochimie, Ecole Polytechnique, CNRS, Université Paris-Saclay, 91128 Palaiseau cedex, France.

[2] Institut de Génétique et de Biologie Moléculaire et Cellulaire (IGBMC), Illkirch, France

[3] Centre National de Recherche Scientifique (CNRS) UMR 7104, Illkirch, France

[4] Institut National de Santé et de Recherche Médicale (INSERM) U964, Illkirch, France

[5] Université de Strasbourg, Illkirch, France

Correspondence to: seraphin@igbmc.fr (Phone: +33-3-88653216) or marc.graille@polytechnique.edu (Phone: +33-1-69334890)

Running title: Pat1 directly interacts with Dcp2 and Xrn1 mRNA decay factors

Keywords: mRNA decapping, eukaryotic mRNA decay, protein-protein interaction, yeast

Two-hybrid assays

The ProQuest two-hybrid assay was used to monitor protein interaction. The desired inserts were amplified by PCR and transferred in the relevant plasmid backbones using the Gateway cloning strategy. Absence of mutation in inserts derived from PCR amplified fragment(s) was ascertained by sequencing. Point mutations were introduced by site-directed mutagenesis in the Gateway Entry plasmid pDONR221, validated by sequencing, and transferred to the relevant backbone. Plasmids are listed in SI Appendix, Table S2. Two-hybrid interaction analyses were done using standard procedure. The ß-galactosidase activity was monitored using the Beta-Glo Assay system (Promega).

Average values and standard-error of the mean of at least two biological duplicates are plotted.

RNA

For analysis of mRNA decay, 1mL aliquots of cells harboring the MFA2pG reporter (1) were collected at the indicated time points. Cell pellets were frozen in liquid nitrogen and stored at -80°C. Yeast total RNA was obtained by hot acid phenol extraction. Northern blot analyses were carried out after agarose gel electrophoresis. The reporter RNA was detected using a radiolabeled oligo(C) probe oRP121 (2). Signals were measured and quantified using PhosphorImager (GE Healthcare). The mRNA half-lives were calculated using the best fit to an exponential decay. scR1 RNA, detected with a specific radiolabeled probe (OBS144 5' TCTAGCCGCGAGGAAGGA 3'), was used as loading control.

Western blot analysis

Yeast strains were grown overnight in YPDA medium and 4OD units equivalent were taken to prepare total yeast extract as described previously (3). For detection a rabbit serum containing polyclonal antibodies generated against a fragment of Pat1 was used (1:1000; kind gift from F. Wyers (4)). As loading control, the endogenous Stm1 protein was detected using polyclonal anti-Stm1 antibody (1:5000; kind gift from F. Wyers).

Cloning, expression and purification of ScPat1C

The coding sequence of *Saccharomyces cerevisiae* Pat1 C-terminal domain (referred as Pat1C) encompassing residues 435 to 796 was amplified from yeast *Saccharomyces cerevisiae* S288C genomic DNA using oligonucleotides oMG47 and oMG52 (SI Appendix, Table S3 for oligonucleotides details) and inserted into pnEA-3CH vector (kind gift from C. Romier, IGBMC, Illkirch, France), yielding plasmid pMG643. The pMG754 plasmid encoding the His_6-Pat1C I724R/ I731R mutant was obtained by one-step site-directed mutagenesis of pMG643 using oligonucleotides oMG265 and oMG266, according to Zheng *et al.* (5). The pBS4527 plasmid containing the Pat1 R721A/R728A/F732A/E794A mutation was constructed by 3 successive rounds of site-directed mutagenesis using oligonucleotides OBS5017 and OBS5019-OBS5023. The fragment encoding for the Pat1C R721A/R728A/F732A/E794A mutant was amplified from this plasmid template using oligonucleotides oMG119 and oMG173 (SI Appendix, Table S3) and inserted into pET21a vector to yield plasmid pMG616 (SI Appendix, Table S2). Absence of other mutations was verified by sequencing.

The various Pat1C domains (His-tagged WT and mutants) used in this study were produced and purified as previously described (6). The untagged WT Pat1C domain was purified on a NiNTA column (Qiagen). Eluted protein was incubated overnight with 3C-His_6 protease in buffer A (20 mM Tris-HCl pH 8, 200 mM NaCl). The His-tagged 3C protease and uncleaved protein were removed by incubation with NiNTA resin. The untagged Pat1C domain was present in the flow-through and further purified by size-exclusion chromatography on Superdex 75 16/60 column (GE Healthcare) pre-equilibrated with buffer A.

Cloning, expression and purification of Dcp2 and Xrn1 GST fusion proteins

DNA sequences encoding individual HLMs from Dcp2 or Xrn1 as well as Dcp2 [435-508] were amplified from *Saccharomyces cerevisiae* S288C genomic DNA using oligonucleotides oMG185-186, oMG235-254 and oMG338-339 (SI Appendix, Table S3) and then inserted in pGEX-6P-1 expression vectors (see SI Appendix, Table S2 for plasmid listing). GST-HLMs fusions were then expressed in *E. coli* BL21 (DE3) in 2YT medium supplemented with ampicillin at 50 µg/mL. At OD_{600} = 0.8, protein expression was induced at 37°C for 3 h by adding 50 µg/mL IPTG. Cells were harvested by centrifugation and resuspended in 40 mL of buffer A supplemented with protease inhibitor cocktail. Cell lysis was performed by sonication.

All GST-HLMs constructs were purified on a Glutathione Sepharose™ 4B (GE Healthcare) column according to manufacturer instructions, and then on a Superdex™ 75 16/60 size exclusion column (GE Healthcare) equilibrated in buffer A.

Cloning, expression and purification of GST-Dcp1:Dcp2 complexes

The Dcp1 coding sequence was amplified from plasmid pBS2246 containing the cloned *S. cerevisiae* Dcp1 coding sequence using OBS5397 and OBS5398. The PCR product was digested with BamHI and SalI and cloned in BamHI/SalI digested pGEX6P1 to give pBS4576. The Dcp2 [1-315]-His_6 coding sequence was amplified with oligonucleotides OBS5884 and OBS6664 from *S. cerevisiae* genomic DNA, and Dcp2 [1-460]-His_6 with OBS5884 and OBS6665. The PCR products were digested with NotI and SalI and cloned in NotI/SalI digested pBS4576 giving pBS5135 and pBS5136, respectively. Absence of mutations was verified by sequencing.

Expression of GST-Dcp1/Dcp2-His_6 complexes of different length, was carried out in *E. coli*

BL21(DE3) Codon$^+$ (Novagen) in 1 L of auto-inducible terrific broth media (ForMedium AIMTB0260) supplemented with ampicillin at 100 µg/mL and chloramphenicol at 25 µg/mL. At OD_{600}=0.8, cells were transferred at 25°C for 20 h. Bacteria were harvested by centrifugation and resuspended in 40 mL of Buffer B (20 mM Tris-HCl pH 8, 200 mM NaCl pH8, 5mM ß-mercaptoethanol and 1mM $MgCl_2$) supplemented with 20 mM imidazole. Cell lysis was performed by sonication. These GST-Dcp1:Dcp2-His_6 constructs were purified on a NiNTA column (Qiagen), followed by an overnight 3C protease digestion in order to remove GST, an heparin column (GE Healthcare) and finally a Superdex200 16/60 size exclusion column (GE Healthcare) in buffer B.

Crystallization and structures determination

Prior to crystallization trials, the Pat1C Q706A/L713A mutant domain (10 mg/mL) was incubated with a two-fold molar excess of either Dcp2 HLM2 (Dcp2[435-451]), HLM3 (Dcp2[484-500]) or HLM10 (Dcp2[954-970]) peptides. The Pat1C(Q706A/L713A):Dcp2[HLM3] complex was crystallized using vapor diffusion method in hanging drop at 24°C, by adding 1 µL of Pat1C(Q706A/L713A):Dcp2[HLM3] mix in buffer B to an equal volume of crystallization solution (200mM $MgCl_2$, 24% PEG 3350). Crystals of Pat1C(Q706A/L713A):Dcp2[HLM2] and Pat1C(Q706A/L713A):Dcp2[HLM10] complexes were obtained in the same conditions by streak-seeding using Pat1C(Q706A/L713A):Dcp2[HLM3] crystals. Crystals were cryo-protected by transfer into their crystallization condition supplemented with the corresponding peptide (two-fold molar excess) and with progressively higher ethylene glycol concentration up to 30% and then flash-frozen in liquid nitrogen.

All datasets were collected on beam-lines Proxima-1 and Proxima-2 (Synchrotron SOLEIL, Saint-Aubin, France). Data indexing and processing were performed with the program XDS (7). All these crystals belong to space group I222 with two copies of Pat1C-HLM complex per asymmetric unit. The structures were solved by molecular replacement using PHASER MR (8) from the CCP4 program suite, searching for two copies of free Pat1C structure (6) by asymmetric unit. Successive building/refinement cycles were carried out using the COOT (9) and the BUSTER (10) programs. Statistics on data collection and structure refinement are summarized in SI Appendix, Table S4.

The final model for Pat1C:HLM2 complex contains Pat1C residues 468 to 644 and 658 to 796 (protomer A) and residues 468 to 600, 604 to 647 and 659 to 795 (protomer B) as well as Dcp2

residues 437 to 450 (protomer C) and 438 to 449 (protomer D). No water molecules were modelled because of the poor quality of the electron density maps resulting from highly anisotropic diffraction data. The final model for Pat1C:HLM3 complex contains Pat1C residues 472 to 646 and 660 to 796 (protomer A) and residues 473 to 599, 604 to 653 and 656 to 796 (protomer B) as well as Dcp2 residues 484 to 500 (protomers C and D), nine molecules of ethylene glycol used as cryoprotectant, one Mg^{2+} and two Cl^{-} ions from the crystallization conditions and 143 water molecules. For Pat1C:HLM10 complex, Pat1C residues 468 to 645 and 659 to796 (protomer A) and residues 473 to 517 and 521 to 796 (protomer B) could be modeled into the 2Fo-Fc electron density map, as well as Dcp2 residues 957 to 969 (protomer C) and 958 to 970 (protomer D), thirteen molecules of ethylene glycol used as cryoprotectant, one Mg^{2+} ion from the crystallization condition, one Tris molecule from the protein buffer and 196 water molecules.

Pull-down assays

Pull-down experiments were performed by mixing either 1.13 nmol of His-tagged Pat1C with an equal molar amount of GST-HLMs fusions or 280 pmol of His-tagged Dcp2 in complex with Dcp1 with an equal molar amount of untagged Pat1C. Binding buffer (20 mM Tris-HCl pH 7.5, 100 mM NaCl, 50 mM Imidazole, 10% Glycerol) was added to a final volume of 60 µL. The reaction mixtures were incubated on ice for 1 hour. 10 µL was withdrawn as “input” fraction for SDS-PAGE analysis. The remaining 50 µL were incubated with 500 µg of HisPur™ Ni-NTA Magnetic Beads (Thermo Scientific) equilibrated in binding buffer to a final volume of 200 µL at 4°C for 2 hours. Beads were washed three times with 500 µL of Binding Buffer. Bound proteins were eluted with 250 mM Imidazole. Samples were resolved on 15% SDS-PAGE and visualized by Coomassie blue staining.

Fluorescence anisotropy

Unlabeled and FITC-labeled peptides were synthesized by the IGBMC Peptide Synthesis facility using the Fmoc chemistry. Crude peptide products were purified by reverse phase high performance liquid chromatography (HPLC). Quality and purity of the final products were assessed by HPLC and mass spectrometry.

Affinities between Pat1C and the different HLM peptides were quantified by fluorescence anisotropy using a FP8300 spectrofluorimeter (Jasco) at 20°C. Increasing amounts of Pat1C (0 to 30-40 µM) were added into a solution composed of 20 mM Tris-HCl pH 8, 200 mM NaCl and

containing the respective HLMs peptide N-terminally fused to FITC (HLM-FITC) at a concentration of 10 nM in a 400 µL final volume. $Kd_{HLM\text{-}FITC}$ and dR_{max} (maximum value of anisotropy difference) were calculated by fitting experimental curves with equation (A) using the program OriginLabs:

$$(A) \qquad dR=(dR_{max} * [Pat1C])/(Kd_{HLM\text{-}FITC} + [Pat1C])$$

where dR is the anisotropy difference for a given Pat1C concentration ([Pat1C]).

Control experiments were performed by chasing HLM2 fluorescent peptide (10 nM) by increasing concentrations of the corresponding unlabeled peptide and dissociation constant (Kd_{HLM}) was determined by fitting experimental curve with equation (B):

$$(B) \qquad dR=(dR_{max} * [Pat1C])/([Pat1C] + Kd_{HLM\text{-}FITC}(([HLM]/Kd_{HLM})+1))$$

where dR is the anisotropy difference for a given concentration of unlabeled HLM peptide ([HLM]).

SI Appendix, Supplementary Figures

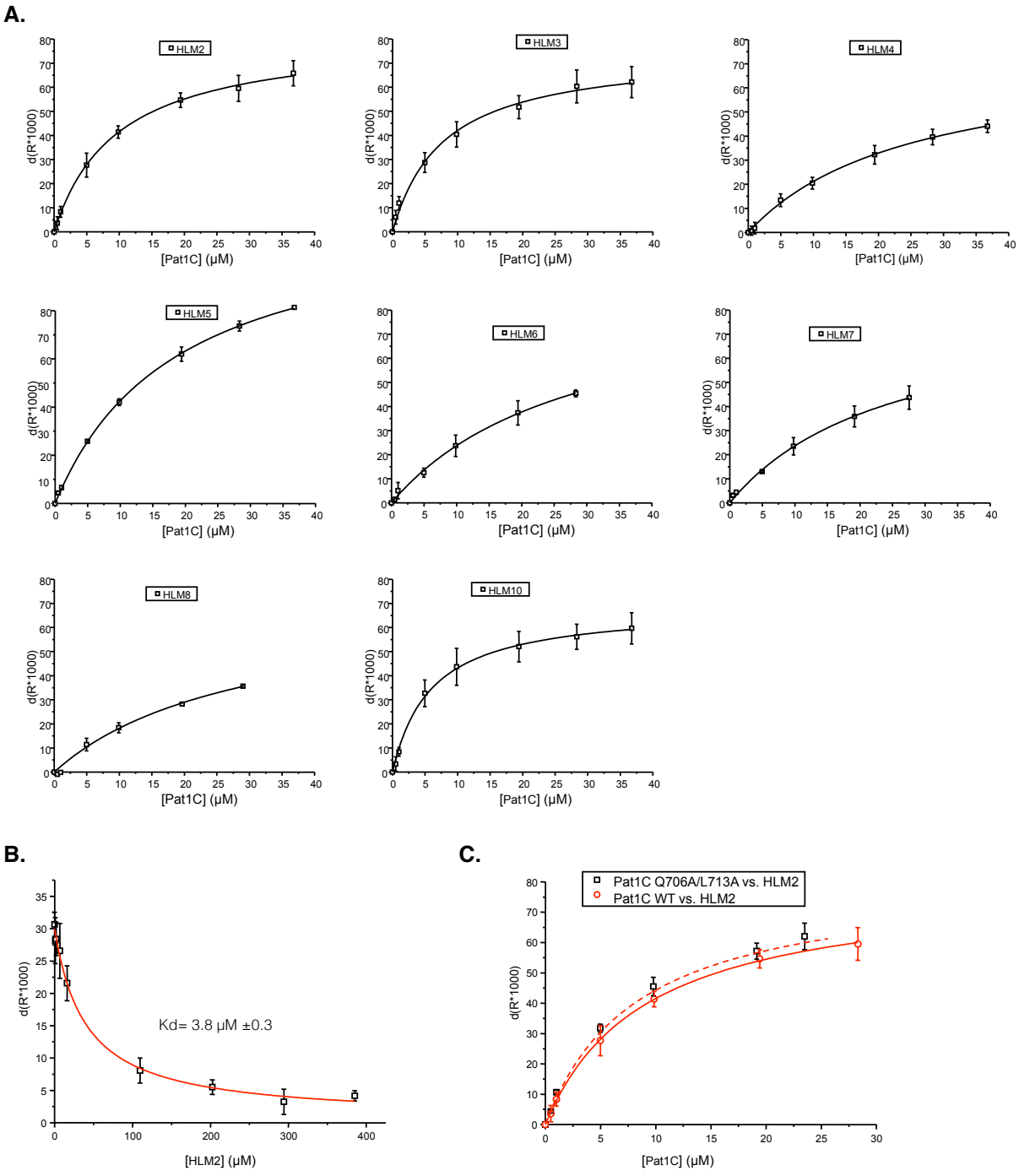

Figure S1: Binding of Dcp2 HLM peptides to Pat1C.

A. Fluorescence anisotropy analyses of Dcp2 HLM peptides binding to Pat1C. FITC-labeled HLM peptides (10 nM) were incubated with increasing amount of purified recombinant yeast Pat1C protein. The graph represents the difference in anisotropy between the free fluorescent peptides and the reaction mix as a function of Pat1C concentration. The curves obtained after fitting of the experimental data with equation (A) from the materials and methods section, are shown as a solid line. Error bars were calculated from triplicate experiments.

B. Chase experiments of an FITC-labeled HLM2 peptide (10 nM) bound to Pat1 (20 μM) by an unlabeled HLM2 peptide. The curve obtained after fitting of the experimental data with equation (B) from the materials and methods section, is shown as a solid red line. Error bars

were calculated from triplicate experiments.

C. Titration of a FITC-HLM2 peptide from Dcp2 by either the Pat1C WT domain (red open circles) or the Pat1C Q706A/L713A mutant (black open squares). The curves obtained after fitting of the experimental data with equation (A) from the materials and methods section, are shown as a solid (WT) or dashed (Q706A/L713A) red lines. Error bars were calculated from triplicate experiments.

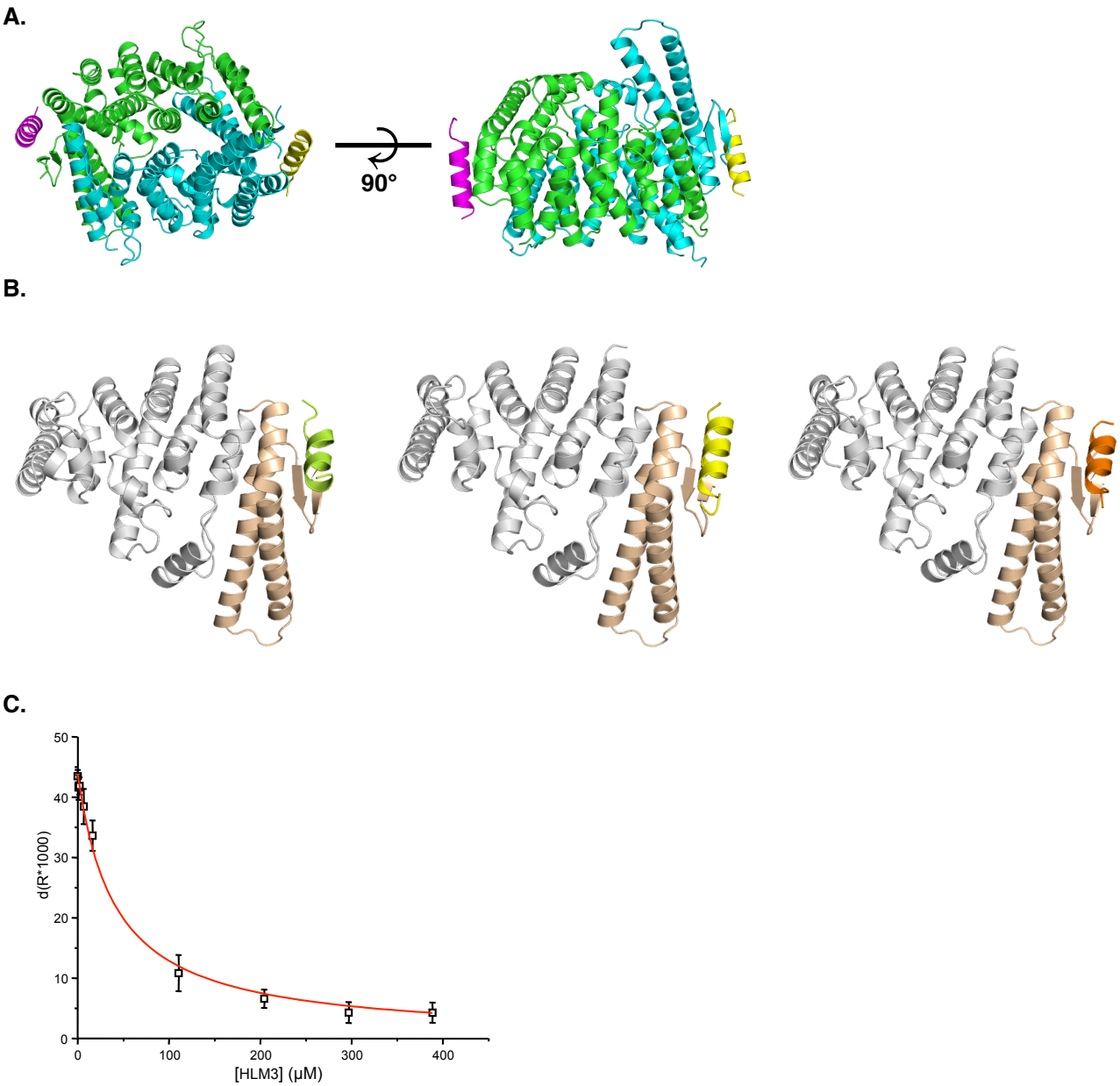

Figure S2: Dcp2 HLM peptides bind to the same region on Pat1C.

A. Ribbon representation of Pat1C-HLM dimers present in the asymmetric unit illustrated for Pat1C-HLM3 complex. Pat1C monomers are colored in green and cyan while Dcp2 HLM peptides are in magenta and yellow. The right panel is rotated 90°C along the horizontal axis relative to the left panel.

B. Ribbon representation of complexes formed between Pat1C (grey) and Dcp2 HLM2 (left), HLM3 (middle) and HLM10 (right) peptides. The Dcp2 HLM2, HLM3 and HLM10 peptides are colored green, yellow and orange, respectively. The fungi-specific Pat1 region is colored in beige.

C. Chase experiments of a FITC-labeled HLM2 peptide (10 nM) bound to Pat1 (20 µM) by an unlabeled HLM3 peptide. The curve obtained after fitting of the experimental data with equation (B) from the materials and methods section, is shown as a solid red line. Error bars were calculated from triplicate experiments.

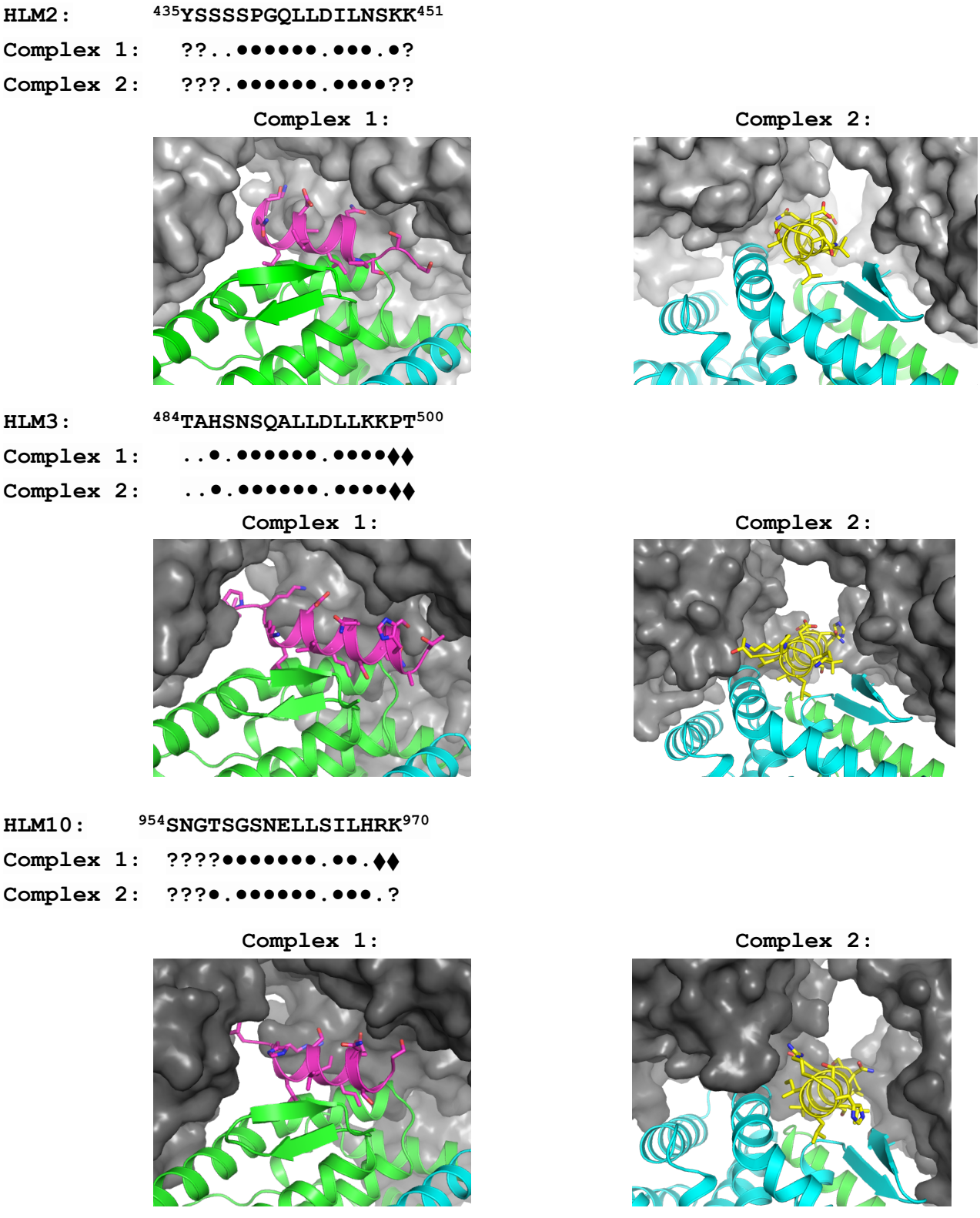

Figure S3: Crystal packing and Dcp2 HLM peptides.

Crystal packing representation in the vicinity of Dcp2 HLM peptides in both Pat1-HLM complexes of the asymmetric unit (complexes 1 and 2 with Dcp2 HLM peptides shown in magenta and yellow, respectively). ScPat1C molecules contacting HLM peptides in biologically relevant complexes are shown in green and cyan ribbons. ScPat1C molecules contacting HLM peptides due to the crystal packing are shown by grey surfaces.

The sequence of each HLM peptide co-crystallized with ScPat1C is given with the following code: residues not present in the final model due to the absence of electron density map (?); residues making no contact with Pat1 (.); residues directly involved in the interaction with Pat1 (closed black circles); residues engaged in crystal packing (closed back diamonds).
For each of the six Pat1 - Dcp2 HLM complexes (two per HLM peptide), this figure shows the Pat1 proteins present in the close vicinity of the HLM peptide (colored in magenta or yellow for complexes 1 and 2, respectively) in the asymmetric unit (cartoon representation in cyan and green) or in neighboring asymmetric units (grey surface).

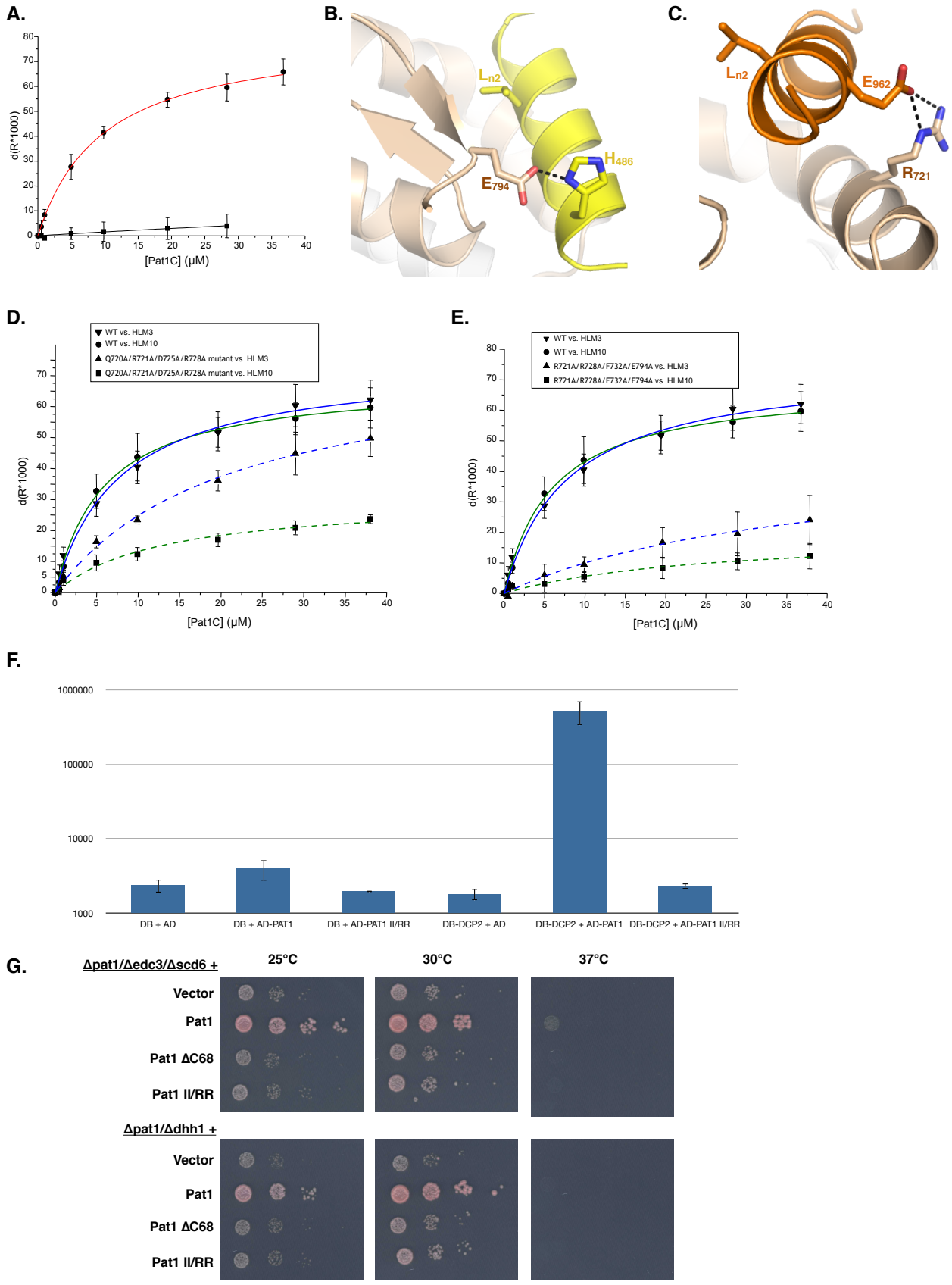

Figure S4: Mutants affecting Pat1C-Dcp2 HLM interaction.

A. Titration of WT (closed circles) or L443A-L444A (closed squares) FITC-HLM2 peptides from Dcp2 by the Pat1C domain. The curves obtained after fitting of the experimental data with equation (A) from the materials and methods section, are shown as a solid (WT) or dashed

(Q706A/L713A) lines. Error bars were calculated from triplicate experiments.

B. Ribbon representation of the Pat1C-HLM3 complex. The electrostatic interaction formed between Pat1C E794 and H486 from Dcp2 HLM3 is depicted by a black dashed line. L_{n2} side chain from the HLM motif is shown as stick as a reference mark.

C. Ribbon representation of the Pat1C-HLM10 complex. The electrostatic interaction formed between Pat1C R721 and E962 from Dcp2 HLM10 is depicted by a black dashed line. L_{n2} side chain from the HLM motif is shown as stick as a reference mark.

D. Titration of HLM3 or HLM10 peptides from Dcp2 by either Pat1C WT or Q720A/R721A/D725A/R728A mutant. The curves obtained after fitting of the experimental data with equation (A) from the materials and methods section, are shown as a solid (WT) or dashed (Q720A/R721A/D725A/R728A) lines. Fitted curves for HLM3 or HLM10 peptides are colored blue or green, respectively. Error bars were calculated from triplicate experiments.

E. Titration of HLM3 or HLM10 peptides from Dcp2 by either Pat1C WT or R721A/R728A/F732A/E794A mutant. The curves obtained after fitting of the experimental data with equation (A) from the materials and methods section, are shown as a solid (WT) or dashed (R721A/R728A/F732A/E794A) lines. Fitted curves for HLM3 or HLM10 peptides are colored blue or green, respectively. Error bars were calculated from triplicate experiments.

F. Effect of the II/RR Pat1 mutation on Dcp2 binding as monitored by yeast two-hybrid assay.

G. Growth analysis of PAT1 mutants in *pat1Δ/dhh1Δ* and *pat1Δ/edc3Δ/scd6Δ* strains. Serial dilutions of the different strains transformed with vector, a plasmid encoding wild type Pat1, Pat1ΔC68, or Pat1 II/RR ScPat1 mutants were spotted on -TRP plates and incubated at the indicated temperatures for 3 days.

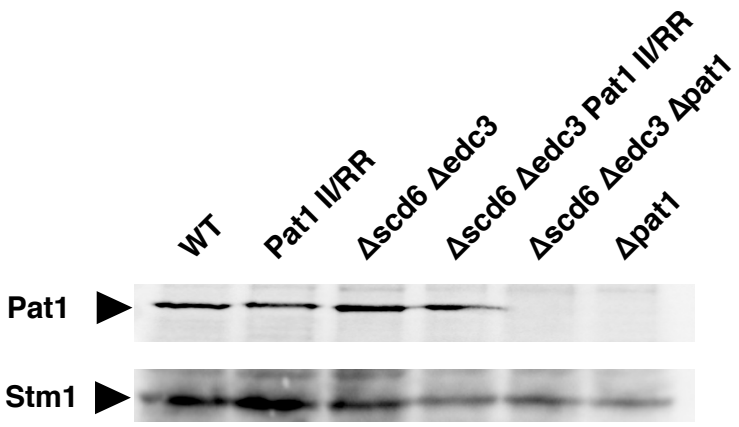

Figure S5: Western blot analysis of Pat1 levels in strains with the indicated genotypes. The yeast Stm1 protein was used as a loading control.

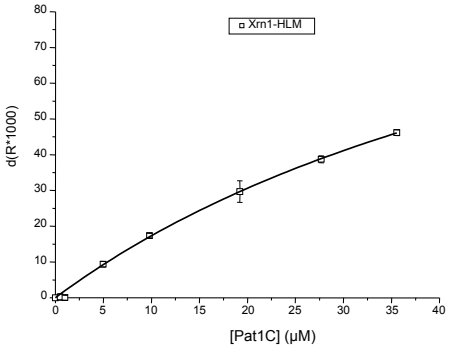

Figure S6: Xrn1 HLM peptide binding to Pat1C.

Fluorescence anisotropy analyses of Xrn1 HLM peptide binding to Pat1C. FITC-labeled HLM peptide (10 nM) was incubated with increasing amount of purified recombinant yeast Pat1C protein. The graph represents the difference in anisotropy between the free fluorescent peptides and the reaction mix as a function of Pat1C concentration. The curves obtained after fitting of the experimental data with equation (A) from the materials and methods section, are shown as a solid line. Error bars were calculated from triplicate experiments.

SI Appendix, Supplementary Tables

Table S1 : Yeast strains

Name	Genotype	Reference	Use
BMA64	MATα; ura3-1; Δtrp1; ade2-1; leu2-3,112; his3-11,15	(11)	Functional assays
YFW168	MATa; ura3-1; Δtrp1; ade2-1; leu2-3;112; his3-11,15; Δpat1::HIS3; Δdhh1::Kan^R	(6)	Functional assays
BSY1133	MATa, ade2-1, his3-11, -15, leu2-3, -112, trp1-1, ura3-1 Δpat1::HIS3	This work	Functional assays
BSY2601	MATa; ura3-1 or ura3-52; trp1-1 or Δtrp1; ade2-1; leu2-3,112; his3-11,15; Δpat1::HIS3; Δscd6::Kan^R; Δedc3::Nat^R	(6)	Functional assays
BSY2602	MATα; ura3-1 or ura3-52; trp1-1 or Δtrp1; ade2-1; leu2-3,112; his3-11,15; Δpat1::HIS3; Δscd6::Kan^R; Δedc3::Nat^R	(6)	Functional assays
BSY3007	MATα; ura3-1; Δtrp1; ade2-1; leu2-3,112; his3-11,15; dcp2(1-300)::VSV-KAN^R	This work	Functional assays
BSY3089	MATα; ura3-1; Δtrp1; ade2-1; leu2-3,112; his3-11,15; pat1 I724R/I731R	This work	Functional assays
BSY3113	MATα; ade 2-1; his3-11,15; leu2-3,112; Δtrp1, ura3-1, can1-100, Δedc3::NAT^R; Δscd6::Kan^R	This work	Functional assays
BSY3112	MATα; ade 2-1; his3-11,15; leu2-3,112; Δtrp1, ura3-1, can1-100, Δedc3::NAT^R; Δscd6::Kan^R; pat1 I724R/I731R	This work	Functional assays
MAV203	MATα; leu2-3,112; trp1-901; his3Δ200; ade2-101; gal4Δ; gal80Δ; SPAL10::URA3; GAL1::lacZ; HIS3UAS GAL1::HIS3@LYS2; can1^R; cyh2^R	Invitrogen	Two-hybrid
BSY3010	MATα; leu2-3,112; trp1-901; his3Δ200; ade2-101; gal4Δ; gal80Δ; SPAL10::URA3; GAL1::lacZ; HIS3UAS GAL1::HIS3@LYS2; can1^R; cyh2^R ; dcp2 1-247 ::kanMX	This work	Two-hybrid
BSY3011	MATα; leu2-3,112; trp1-901; his3Δ200; ade2-101; gal4Δ; gal80Δ; SPAL10::URA3; GAL1::lacZ; HIS3UAS GAL1::HIS3@LYS2; can1^R; cyh2^R ; dcp2 1-300 ::kanMX	This work	Two-hybrid
BSY3012	MATα; leu2-3,112; trp1-901; his3Δ200; ade2-101; gal4Δ; gal80Δ; SPAL10::URA3; GAL1::lacZ; HIS3UAS GAL1::HIS3@LYS2; can1^R; cyh2^R ; dcp2 1-663 ::kanMX	This work	Two-hybrid

Table S2 : Plasmids

Name	Description	Reference or oligonucleotides
pGEX6P1		Amersham
pBS4576	GST-yDCP1 (pGEX-6P-1)	OBS5397/OBS5398
pBS5135	GST-yDCP1/DCP2[1-315]-6HIS (pGEX-6P-1)	OBS5884/OBS6664
pBS5136	GST-yDCP1/DCP2[1-460]-6HIS (pGEX-6P-1)	OBS5884/OBS6665
pBS2379	pFA6a-KanMX6	(12)
pCAS	CAS9 and gRNA LYP1	(13)
pBS5391	CAS9 and gRNA PAT1	OBS6969/OBS6970
pBS2368	pDEST32 yEDC3	Gift from N.Cougot
pBS3892	pDONR221 yDHH1	OBS4230/OBS4231
pBS3909	pDEST32 yDHH1	This work
pBS2371	pDEST32 yDCP2	Gift from N.Cougot
pBS2411	pEXP-AD502	Invitrogen
pBS2410	pDB-Leu	Invitrogen
pBS2374	pDEST22 yPAT1	Gift from N.Cougot
pBS5131	pDONR221 yPAT1 I724R/I731R	OBS6661/OBS6662
pBS4907	pDEST22 yPAT1 DC68	(6)
pBS5133	pDEST22 yPAT1 I724R/I731R	This work
pBS2371	pDEST32 yDCP2	Gift from N.Cougot
pBS3841	pDONR221 yDCP2 [436-663]	OBS4108/OBS4107
pBS3859	pDEST32 yDCP2 [436-663]	This work
pBS3845	pDONR221 yDCP2 [368-460]	OBS4110/OBS4111
pBS3867	pDEST32 yDCP2 [368-460]	This work
pBS5125	pDONR221 yDCP2 [450-663]	OBS6644/OBS4107
pBS5127	pDEST32 yDCP2 [450-663]	This work
pBS5141	pDONR221 yDCP2 3[68-460] HLM2*	OBS6682/OBS6646
pBS5144	pDEST32 yDCP2 [368-460] HLM2*	This work
pBS5175	pDONR221 yDCP2 [450-663] HLM3*	OBS6647/OBS6648
pBS5187	pDEST32 yDCP2 [450-663] HLM3*	This work
pRS414	Shuttling vector with TRP1 marker	(14)
pBS4357	pRS414 yPAT1	(6)
pBS4421	pRS414 yPAT1 ΔC68	(6)
pBS5186	pRS414 yPAT1 I724R/I731R	This work

pBS4527	pRS414 yPAT1 R721A/R728A/F732A/E794A	This work
pBS5441	pDONR221 yXRN1 [1-1456]	OBS4232/OBS7063
pBS5453	pDEST32 yXRN1 [1-1456]	This work
pBS5462	pDONR221 yXRN1 [1-1456] HLM*	OBS7080/OBS7081
pBS5480	pDEST32 yXRN1 [1-1456] HLM*	This work
RP485	MFA2pG reporter with URA3 marker	(1)
pMG606	6His-yPat1[435-796] Q706A/L713A (pET-21a)	(6)
pMG610	6His-yPat1[435-796] Q720A/R721A/D725A/R728A (pET-21a)	(6)
pMG616	6His-yPat1[435-796] R721A/R728A/F732A/E794A (pET-21a)	oMG119/oMG173
pMG621	GST-yDcp2[435-508] (pGEX-6P-1)	oMG185/oMG186
pMG631	GST-yDcp2[433-457]HLM2 (pGEX-6P-1)	oMG237/oMG238
pMG632	GST-yDcp2[482-506]HLM3 (pGEX-6P-1)	oMG239/oMG240
pMG633	GST-yDcp2[785-819]HLM5 (pGEX-6P-1)	oMG243/oMG244
pMG634	GST-yDcp2[817-841]HLM6 (pGEX-6P-1)	oMG245/oMG246
pMG635	GST-yDcp2[923-947]HLM9 (pGEX-6P-1)	oMG251/oMG252
pMG636	GST-yDcp2[952-970]HLM10 (pGEX-6P-1)	oMG253/oMG254
pMG637	GST-yDcp2[263-287]HLM1 (pGEX-6P-1)	oMG235/oMG236
pMG643	6His-yPat1[435-796] (pnEA-3CH)	oMG47/oMG52
pMG677	GST-yDcp2[862-886]HLM7 (pGEX-6P-1)	oMG247/oMG248
pMG678	GST-yDcp2[887-911]HLM8 (pGEX-6P-1)	oMG249/oMG250
pMG680	GST-yDcp2[723-747]HLM4 (pGEX-6P-1)	oMG241/oMG242
pMG754	6His-yPat1[435-796] I724R/I731R (pnEA-3CH)	oMG265/oMG266
pMG761	GST-yXrn1 [1277-1301] (pGEX-6P-1)	oMG338/oMG339

For *E. coli* over-expression plasmids, the plasmid backbone used for cloning is indicated into brackets.

Table S3 : Oligonucleotides

Name	Sequence
oMG47	GGATATCCATATGTCTTCAGGGTCCTCCTCT
oMG52	GGGGGATCCTTACTTTAGTTCTGATATTTCACC
oMG119	TTTTTGCGGCCGCTTACTTTAGTTCTGATATTTCACCATCG
oMG173	TTTTTGCGGCCGCTTACTTTAGTGCTGATATTTCACCATCG
oMG185	GGGAAGGATCCAGCAGCTCCTCCCCTGGGC
oMG186	TTTTTGCGGCCGC TTA GGAAGCGTGTATCTTCTGCGA
oMG235	GACGGATCCAAGGAGGAGCAGATTGA
oMG236	CATGCGGCCGCTCAATTATTACTGTTAGCTTGCA
oMG237	GACGGATCCTCTGGTTACAGCAGCTC
oMG238	CATGCGGCCGCTCATTGCACGTTGCTGTCAG
oMG239	GACGGATCCGATGAAACTGCTCATTCAA
oMG240	CATGCGGCCGCTCAGTGTATCTTCTGCGATGA
oMG241	GACGGATCCTCAAGCTCCAATGTGTCT
oMG242	CATGCGGCCGCTCATGAAGATACAGTAGAGGAA
oMG243	GACGGATCCTCAAGTATAAACGATGCGA
oMG244	CATGCGGCCGCTCATGGTGCTGTAATGTCTTT
oMG245	GACGGATCCTCATACTCGCAGAAAAATT
oMG246	CATGCGGCCGCTCAGCGAGGGTACCCG
oMG247	GACGGATCCAATCAAGAATTAGATAAGAA
oMG248	CATGCGGCCGCTCACTCATACCCATCATTAA
oMG249	GACGGATCCAATATTTCAAATAAGGACAG
oMG250	CATGCGGCCGCTCAATTGAAGGCGCTGCTG
oMG251	GACGGATCCGCATCTGATAACAACGAA
oMG252	CATGCGGCCGCTCACTCATTTATTGCACTAGAC
oMG253	GACGGATCCGTCCGTTCGAATGG
oMG254	CATGCGGCCGCTCACTTCCTATGCAAA
oMG265	GAATCATTAGGGATGAAGTACGTGATGAAAGGTTTGCCAC
oMG266	GTGGCAAACCTTTCATCACGTACTTCATCCCTAATGATTC
oMG338	CCCGGATCCGAAAAACTGAGAAAA
oMG339	GGGGCGGCCGCTTATTCAGAATTCTTTTC
OBS144	TCTAGCCGCGAGGAAGGA
OBS5017	AAACCACCAGGCCATCATTATTGATGAAG

OBS5019	ATAATGATGGCCTGGTGGTTTAGCTTTCC
OBS5020	AATATCAGCGCTAAAGTAAGATTTTTCCTG
OBS5021	TTACTTTAGCGCTGATATTTCACCATCGCG
OBS5022	TGAAGTAGCTGATGAAATCGCTGCCACTATTAACG
OBS5023	GTGGCAGCGATTTCATCAGCTACTTCATCAATAATG
OBS6649	GTAATAATAATGCGGTCTCCAACGGACAGGTACCCTCGAGCCAAGAGTGAC GGATCCCCGGGTTAATTAA
OBS6650	CATTTACAGTGTGTCTATAAAACGTATAACACTTATTCTT GAATTCGAGCTCGTTTAAAC
OBS6651	GGTTAAGGCATCAGAGGCAAATAAAAAATGAAGATCAATTGTGACGGATCC CCGGGTTAATTAA
OBS6652	GACAACTCCAAATTAATTAGCCAAGATATTTTAAAAGAGAACTGACGGATCC CCGGGTTAATTAA
OBS5397	GCGCGGATCCATGACCGGAGCAGCAACTGCAGCA
OBS5398	GCGCGTCGACTCAAGCAAAAGAATCTTTTGGCTC
OBS5884	GACTGTCGACTAAGGAGGATATATATGTCACTGCCGCTACGACAC
OBS6664	GACTGCGGCCGCTCAGTGATGGTGATGGTGATGCTTCTGTTGGTTGTGTTC
OBS6665	GATCGCGGCCGCTCAGTGATGGTGATGGTGATGTTTGCTTGATTGCACGTTG CTG
OBS6969	CTTTGCCACTATTAACGAGGGTTTTAGAGCTAGAAATAGC
OBS6970	CCTCGTTAATAGTGGCAAAGAAAGTCCCATTCGCCACCCG
OBS6971	GCTAGTTTAGCACTAAGTGGAAAGCTAAACCACCAGAGAATCATTCGCGAT GAAGTACGTGATGAACGTTTTGCCACTATTAACGAGGCCGAGACCTTACAA AAGAAAGAGAAAG
OBS6972	CTTTCTCTTTCTTTTGTAAGGTCTCGGCCTCGTTAATAGTGGCAAAACGT TCATCACGTACTTCATCGCGAATGATTCTCTGGTGGTTTAGCTTTCCACT TAGTGCTAAACTAGC
OBS4230	GGGGACAAGTTTGTACAAAAAAGCAGGCTTCATGGGTTCCATCAATAATAAC TTC
OBS4231	GGGGACCACTTTGTACAAGAAAGCTGGGTCTTAATACTGGGGTTGTGACTG
OBS6661	GAGAATCATTCGCGATGAAGTACGTGATGAACGTTTTGCCACTATTAACGAG
OBS6662	GTGGCAAAACGTTCATCACGTACTTCATCGCGAATGATTCTCTGGTGGTTTA G
OBS4108	GGGGACAAGTTTGTACAAAAAAGCAGGCTTCAGCAGCTCCTCCCCTGGGCA G
OBS4107	GGGGACCACTTTGTACAAGAAAGCTGGGTCCTAGTTCTCTTTTAAAATATCT TG
OBS4110	GGGGACAAGTTTGTACAAAAAAGCAGGCTTCCCTTTTGCACCTTTCCCATTT
OBS4111	GGGGACCACTTTGTACAAGAAAGCTGGGTCCTATTTGCTTGATTGCACGTTG CA

OBS6644	GGGGACAAGTTTGTACAAAAAAGCAGGCTTCAAAAAGCCTGACAGCAACG TG
OBS6682	AGCTCCTCCCCTGGGCAGGCCGCCGATATACTAAATTCGAAAAAGCCTGACA GCAACGT
OBS6646	CGAATTTAGTATATCGGCGGCCTGCCCAGGGGAGGAGCTGCTGTAACCAGA GTCCCTCGG
OBS6647	TCAAACTCTCAAGCTGCCGCCGATTTGTTGAAAAAACCAACATCATCGCAG AAGATAC
OBS6648	GGTTTTTTTCAACAAATCGGCGGCAGCTTGAGAGTTTGAATGAGCAGTTTCA TCATTAT
OBS4232	GGGGACAAGTTTGTACAAAAAAGCAGGCTTCATGGGTATTCCAAAATTTTTC AGG
OBS7063	GGGGACCACTTTGTACAAGAAAGCTGGGTCCTATTGATCTGAAACATTTGTC ATAG
OBS7080	GAAAGGGCACATGATGCAGCGAATTTTATCAAAAAGGATACCAATGAAAAG AATTC
OBS7081	CCTTTTTGATAAAATTCGCTGCATCATGTGCCCTTTCTTTTCTCAGTTTTTCTT CAGATTG

Table S4: Data collection and refinement statistics.

	Pat1C-HLM2	Pat1C-HLM3	Pat1C-HLM10
Data collection			
Space group	I222	I222	I222
Cell parameters			
a, b, c (Å)	98.3, 116, 122	98.4, 122.9, 127	97.7, 123, 126.6
α, β, γ (°)	90, 90, 90	90, 90, 90	90, 90, 90
Resolution (Å)	50-2.6 (2.75-2.6)	50-2.15 (2.27-2.15)	50-1.9 (2.0-1.9)
Total number of reflections	93829	124317	249938
Total number of unique reflections	21634	41458	59110
Rsym	0.134 (1.51)	0.102 (1.25)	0.06 (1.57)
CC (1/2)	99.6 (54.2)	99.6 (45.9)	99.9 (45.9)
I/σ(I)	6.5 (1)	7.5 (0.94)	12.15 (0.6)
Completeness (%)	99.1 (98.9)	97.3 (93.9)	97.2 (88.4)
Redundancy	4.3	3	4.2
Refinement			
Resolution (Å)	50-2.6	50-2.15	50-1.9
R (%)	25.6	21.2	20.4
Rfree (%)	26.8	24.6	23.5
R.m.s. deviations			
Bond lengths (Å)	0.01	0.01	0.01
Bond angles (°)	1.12	1.07	1.01
PDB code	5LM5	5LMF	5LMG

Numbers in parentheses are for the highest resolution shell.

Supporting Material References

1. Decker CJ & Parker R (1993) A turnover pathway for both stable and unstable mRNAs in yeast: evidence for a requirement for deadenylation. Genes Dev 7(8):1632-1643.
2. Boeck R, Lapeyre B, Brown CE, & Sachs AB (1998) Capped mRNA degradation intermediates accumulate in the yeast spb8-2 mutant. Mol Cell Biol 18(9):5062-5072.
3. Kushnirov VV (2000) Rapid and reliable protein extraction from yeast. Yeast 16(9):857-860.
4. Wyers F, Minet M, Dufour ME, Vo LT, & Lacroute F (2000) Deletion of the PAT1 gene affects translation initiation and suppresses a PAB1 gene deletion in yeast. Mol Cell Biol 20(10): 3538-3549.
5. Zheng L, Baumann U, & Reymond JL (2004) An efficient one-step site-directed and site-saturation mutagenesis protocol. Nucleic Acids Res 32(14):e115.
6. Fourati Z*, et al.* (2014) The C-terminal domain from S. cerevisiae Pat1 displays two conserved regions involved in decapping factor recruitment. PloS one 9(5):e96828.
7. Kabsch W (1993) Automatic processing of rotation diffraction data from crystals of initially unknown symmetry and cell constants. J. Appl. Cryst. 26:795-800.
8. McCoy AJ*, et al.* (2007) Phaser crystallographic software. Journal of Applied Crystallography 40(4):658-674.
9. Emsley P & Cowtan K (2004) Coot: model-building tools for molecular graphics. Acta Crystallogr D Biol Crystallogr 60(Pt 12 Pt 1):2126-2132.
10. Bricogne G*, et al.* (2011) Buster version 2.8.0Cambridge, United Kingdom: Global Phasing Ltd.).
11. Baudin-Baillieu A, Guillemet E, Cullin C, & Lacroute F (1997) Construction of a yeast strain deleted for the TRP1 promoter and coding region that enhances the efficiency of the polymerase chain reaction-disruption method. Yeast 13(4):353-356.
12. Longtine MS*, et al.* (1998) Additional modules for versatile and economical PCR-based gene deletion and modification in Saccharomyces cerevisiae. Yeast 14(10):953-961.
13. Ryan OW*, et al.* (2014) Selection of chromosomal DNA libraries using a multiplex CRISPR system. eLife 3.
14. Sikorski RS & Hieter P (1989) A system of shuttle vectors and yeast host strains designed for efficient manipulation of DNA in Saccharomyces cerevisiae. Genetics 122(1):19-27.